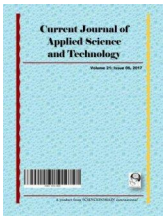

Current Journal of Applied Science and Technology

26(2): 1-24, 2018; Article no.CJAST.37300
ISSN: 2457-1024
(Past name: British Journal of Applied Science & Technology, Past ISSN: 2231-0843, NLM ID: 101664541)

Batch Equilibrium and Effects of Ionic Strength on Kinetic Study of Adsorption of Phenacetin from Aqueous Solution Using Activated Carbon Derived from a Mixture of *Ayous* Sawdust and *Cucurbitaceae* Peelings

Christian Sadeu Ngakou[1], Horace Manga Ngomo[2] and Solomon Gabche Anagho[1,3*]

[1]Laboratory of Noxious Chemistry and Environmental Engineering, Department of Chemistry, Faculty of Science, University of Dschang, P.O.Box 67, Dschang, Cameroon.
[2]Department of Inorganic Chemistry, Faculty of Science, University of Yaoundé I, P.O.Box 812, Yaoundé, Cameroon.
[3]Department of Chemistry, Faculty of Science, University of Bamenda, P.O.Box 39, Bambili, Cameroon.

Authors' contributions

This work was carried out in collaboration between all authors. Authors CSN, HMN and SGA designed the study, performed the statistical analysis, wrote the protocol and wrote the first draft of the manuscript. Authors CSN and SGA managed the analyses of the study. Authors CSN and HMN managed the literature searches. All authors read and approved the final manuscript.

Article Information

DOI: 10.9734/CJAST/2018/37300
Editor(s):
(1) Sahar Ibrahim Hamed Mostafa, Professor, Chemistry Dept., Faculty of Science, Mansoura University, Egypt.
(2) Jesús F. Arteaga, Associate Professor, Department of Chemical Engineering, Physical Chemistry and Organic Chemistry, University of Huelva, Spain.
Reviewers:
(1) Mohammad Isa Mohamadin, Mara University of Technology, Malaysia.
(2) Refaat Ibrahim Nessim, Cairo University, Egypt.
Complete Peer review History: http://www.sciencedomain.org/review-history/23326

Original Research Article

Received 9th October 2017
Accepted 25th January 2018
Published 24th February 2018

ABSTRACT

The present study is based on the adsorption of phenacetin on activated carbon prepared from *ayous* sawdust, *Cucurbitaceae* peelings and the mixture of the two materials using the batch technique. EDX analysis of the activated carbons showed that each one of them was constituted of

**Corresponding author: E-mail: sg_anagho@yahoo.com;*

carbon and oxygen. The mixture of a*yous* sawdust and *Cucurbitaceae* peelings did not show an increase in the percentage of carbon. SEM analysis showed that the mixture showed a change in the nature of pore present in activated carbons. The FT-IR analysis shows after adsorption one peak around 2200 cm^{-1} and the larger peaks near 1100 cm^{-1} are the proof that both activated carbons have adsorbed phenacetin. Adsorption was carried out by variation of the pH, contact time, ionic strength and initial concentration. The equilibrium time was achieved within 2 hours for both activated carbons. The maximum adsorption occurred at pH 2 for all the activated carbons. The adsorbent/adsorbate equilibrium was well described by the pseudo-second-order kinetic model and Langmuir's adsorption model. The ionic strength was investigated using KCl, $MgCl_2$ and $CaCl_2$. The result showed that $CaCl_2$ was the best salt in term of increasing the adsorbed quantities. Using the pseudo-second-order and Elovich kinetic models, it was also observed that $CaCl_2$ increased the initial rate of adsorption while $MgCl_2$ increased the desorption rate constant. This can be attributed to the adsorbed calcium phenacetin complex that is more stable than the magnesium and potassium phenacetin complex. Multi-linearity observed in Weber and Morris diffusion model, implying that more than one mechanism affected the adsorption process and the intraparticle diffusion is not the only process that can control the kinetics of adsorption. We have also found that the mixture of the precursors favor the mass transfer from the solution to the adsorption site inside the activated carbons and their fixation.

Keywords: Activated carbon; kinetics; equilibrium; ionic strength; diffusion; adsorption mechanism; SEM-EDX analysis; phenacetin.

1. INTRODUCTION

The increase of the production of generic drugs and the lack of appropriate treatment systems for effluents from pharmaceutical industries is responsible for introducing significant amounts of organic and inorganic pollutants into the environment, thus creating serious environmental problems throughout the world [1-2]. The production of pharmaceuticals has increased rapidly in the last decades, providing better health quality for humans and animals [3]. The presence of these pharmaceuticals in the environment in concentrations in the µg/L or ng/L range poses a threat to aquatic organisms in terms of mutagenicity as well as currently unknown effects to humans because of their different ways of transformation [4]. Wastewater originating from pharmaceutical and animal feedstock industries often found their way into sources of surface water [5]. Of the drugs produced, phenaticin stands out as being highly toxic to the liver, and a consumer of it has a high potential for developing hepatitis and cancer [6]. Phenacetin is metabolized in the liver, mainly to paracetamol which is conjugated and excreted as glucuronide and sulfate. Phenacetin dominated the drug market during the first 50 years of the 20^{th} century. It was the most widely used and prescribed drug in most countries [7]. Because of the excessive use, phenacetin may end up in the environment through manufacturing waste, waste from animal excretion, runoff from animal feeding operations, or leaching from municipal landfills. It is obvious that with its frequent use it should be quite frequently present as a micropollutant in our environment.

Adsorption has been developed as an efficient method for the removal of pollutants from contaminated water. A variety of adsorbents, including clays, zeolites, dried plant parts, agricultural waste biomass, biopolymers, metal oxides, microorganisms, sewage sludge, ash and activated carbon have been used for pollutant removal [8-10]. Cost is an important parameter for comparing adsorbent materials [11]. Activated carbon is considered to be a highly effective adsorbent for removing pollutants from aqueous solution. It is the most important commercial adsorbent with a large surface area, high porosity, adequate pore size distribution and high mechanical strength.

Activated carbons can be produced from different carbonaceous materials such as coal, wood, peat especially lignocellulosic by-products like pinewood, date's stone, cola nut shells, and maize stalks. Activated carbons are increasingly being used to remove organic compounds and heavy metals of environmental concern from waste streams.

In the literature activated carbons are produced mainly from single precursors. Therefore, it is very important to investigate the effect of a mixture of the precursor on the adsorption properties of an activated carbon. Among the

lignocellulosic materials used to produce activated carbon, we have *Cucurbitaceae* peelings and ayous sawdust [12-15]. These two materials are chosen because of their abundance. In Cameroon, for example, the production of *Cucurbitaceae* between 2005 and 2008 was 558.530 tonne [16]. It is important to notice that this production increases with time. Concerning ayous, the production in 2015 was about 7 % of exported wood (about 62.000 m^3). It is important to note that this production does not take into account the exploitation for national use [17]. We can, therefore, see that in Cameroon and in the world at large, these two precursors are available in large quantities.

The aim of this study was to use activated carbons produced from *ayous* sawdust, a forestry waste, and *Cucurbitaceae* peelings, a local agricultural waste, to investigate the removal of phenacetin from aqueous solution using these activated carbons.

2. MATERIALS AND METHODS

2.1 Phenacetin

Phenacetin is an antipyretic/analgesic drug. The one used in this study as adsorbate was provided by Aldrich. The stock solution of phenacetin was prepared by dissolving 250 mg of phenacetin in 100 mL of hot distilled water (75 °C) and then completing to 500 mL with cold distilled water. All working solutions of various concentrations of phenacetin were freshly prepared from this stock solution of 500 mg/L. HCl or NaOH of concentration 0.1 M of was used to adjust the initial pH of the solution. KCl, $MgCl_2$ and $CaCl_2$ were used to study the influence of ionic strength on the adsorption process. All chemicals used were of laboratory grade.

2.2 Adsorbents

Activated carbons used had been prepared using Response Surface Methodology (RSM) in the Laboratory of Noxious Chemistry and Environmental Engineering (LANOCHE) of the University of Dschang, Cameroon [18]. Activated carbons were prepared by activating lignocellulosic precursors with 1 molar phosphoric acid, followed by calcination in a furnace at 450°C for one hour. The activated carbon, B1M was prepared from ayous sawdust by activation with 1 M phosphoric acid, while P1M was prepared from *Cucurbitaceae* peelings and BP1M was prepared from a 1:1 mixture of the two.

2.3 Characterizations

Scanning electron microscopy (SEM), elemental analysis using an energy-dispersed x-ray (EDX), FT-IR, pH of zero point charge and micro-analyzer were applied on the activated carbons to study their surface texture, the development of porosity and the percentage of atoms present in them [19,20].

2.4 Adsorption

Adsorption experiments were carried out by mechanical agitation at room temperature. For each run, 30 mL of phenacetin solution of a known initial concentration between 20-50 mg/L was treated with 50 mg of any of the activated carbons. After agitation, the solution was filtered, and the filtrate analyzed to obtain the concentration of the residual phenacetin by using the UV/Vis spectrophotometer (Jenway, model 6715). Similar measurements were carried out by varying the pH of the solution, ionic strength and the initial concentrations of the solution. The amount (Q_t) of phenacetin adsorbed was calculated using the following expressions:

$$Q_t = \frac{C_o - C_t}{m} V \quad (1)$$

where C_o is the initial concentration of the phenacetin, C_t is the concentration at time t, V is the volume of the solution, and Q_t is the quantity adsorbed at time t while m is the mass of the absorbent.

2.4.1 Effect of initial pH

For each adsorbent, the optimal mass of adsorbent obtained at the end of the preceding study was treated with 30 mL of aqueous solution of 40 mg/L of phenacetin in the pH range of 2 to 7. The pH of the solution was adjustment by adding either HCl or NaOH at a concentration of 0.1 M.

2.4.2 Effect of contact time

To determine the effect of agitation time on the adsorption process, 50 mg of ground adsorbent was agitated in a 30 mL solution of phenacetin of initial concentration 40 mg/L for different contact times varying between 0 and 180 minutes. After each contact time t, the solution was rapidly

filtered and the residual concentration determined by spectrophotometer. The amount (Q_e) of phenacetin adsorbed was calculated by using equation (1).

2.4.3 Ionic strength

To determine the effect of ionic strength on the adsorption process, 50 mg of adsorbent was agitated in a 30 mL solution of phenacetin of initial concentration 40 mg/L containing the salt KCl, $CaCl_2$ or $MgCl_2$; with concentration ranging between 0.005 and 0.03 M. At equilibrium time (2 h), the solution was rapidly filtered and the residual concentration determined by spectrophotometer. The amount (Q_e) of phenacetin adsorbed was calculated by using equation (1).

The concentrations that gave maximum adsorption quantities were used to study the effect of ionic strength on contact time.

2.4.4 Kinetics of adsorption studies

The kinetic experiments were conducted using a series of 30 mL solutions containing known amounts of adsorbent and concentrations of phenacetin. The solutions were vigorously agitated for increasing time intervals. At the end of each interval, the solution was analyzed in order to determine the residual concentration of phenacetin. A number of kinetic models were used to test the fit of the experimental data. These are:

2.4.5 Pseudo-second order

The pseudo-second-order kinetics is expressed as

$$\frac{dQ}{Qt} = K_2 (Q_e\text{-}Q_t)^2 \quad (2)$$

where K_2 is the pseudo-second-order rate constant. For boundary conditions t= 0 to t=t and $Q_t = Q_t$, the integrated form of the equation is:

$$\frac{t}{Q_t} = \frac{1}{Q_e^2 K_2} + \frac{t}{Q_e} \quad (3)$$

If the adsorption rate is defined as $h = Q_t/t$, when t approaches 0, the initial rate of adsorption h_o (mg/g min), is:

$$h_o = K_2 . Q_e^2 \quad (4)$$

h_o represent the initial rate of adsorption [21,22].

2.4.6 Pseudo-first order model

The pseudo-first-order equation is generally expressed as [23]:

$$\frac{dQ}{dt} = K_1(Q_e - Q_t) \quad (5)$$

Where Q_e and Q_t are the adsorption capacity at equilibrium and at time t, respectively (in mg/g) and K_1 is the rate constant for the pseudo-first order adsorption (L/mg.min). After integration and applying boundary conditions equation (5) becomes:

$$\ln(Q_e - Q_t) = ln\, Q_e - K_1 t \quad (6)$$

2.4.7 Elovich kinetic model

One of the most useful models for describing such activated chemical adsorption is the Elovich equation (5), which is given by:

$$\frac{dQ_t}{dt} = \alpha \exp(-\beta Q_t) \quad (7)$$

The linear form of equation (5) is given by:

$$Q_t = \frac{1}{\beta}\ln(\alpha\beta) + \frac{1}{\beta} lnt \quad (8)$$

where α (mg/g.min) represent the initial rate of adsorption and β (mg/g.min) the desorption rate constant [24].

2.4.8 Intraparticle diffusion model

In many adsorption cases, Weber-Morris found that adsorbate uptake varies proportionally with $t^{1/2}$ rather than the contact time t [25]. For example, the rate of adsorption can be given by:

$$Q_t = C + K_{id} t^{0.5} \quad (9)$$

Where C is the boundary layer diffusion effects, and it depicts the boundary layer thickness, while K_{id} (mg/g.min) is the initial rate of adsorption, and it is controlled by intra-particle diffusivity.

2.4.9 Batch equilibrium experiments

For each run, the adsorbent was mixed with 30 mL solution of phenacetin, at different initial concentrations varying from 20 to 50 mg/L. The suspension was stirred for two hours, within which equilibrium was attained and with different activated carbon. The amount of phenacetin adsorbed at equilibrium, Q_e (mg/g) was

calculated using equation (1). Equilibrium data was then fitted by using the isotherms of Langmuir, Freundlich, Jovanovic, Elovich and Kiselev.

2.4.10 The Langmuir isotherm

The Langmuir adsorption isotherm is often used of the equilibrium of the adsorption of solutes from solutions. It is expressed as [26]:

$$Q_e = \frac{Q_m K C_e}{1+KC_e} \quad (10)$$

where, Q_e is the adsorption capacity at the equilibrium concentration (mg/g); C_e is the equilibrium concentration of adsorbate in solution (mg/L), while Q_m is the maximum adsorption capacity (mg/g) and K_L is the Langmuir constant (L/mg). Equation (7) can be rearranged to the linear form as [27]:

$$\frac{C_e}{Q_e} = \frac{1}{KQ_m} + \frac{C_e}{Q_m} \quad (11)$$

The Langmuir separation factor R_L, which is an essential characteristic factor of this isotherm is calculated by using the relation:

$$R_L = \frac{1}{1+C_o K_L} \quad (12)$$

where C_o is the initial concentration of phenacetin, while K_L and Q_m are the Langmuir constant and the maximum adsorption capacity respectively.

2.4.11 Freundlich isotherm

The equation of the Freundlich isotherm is given by:

$$Q_e = K_f C_e^{1/n} \quad (13)$$

The linear form of equation (10) is given by:

$$lnQ_e = lnK_f + {}^1/_n \, lnC_e \quad (14)$$

The plot of lnQ_e versus lnC_e allows the different constants in the equation to be determined [27, 28].

2.4.12 Jovanivic isotherm model

This model is similar to that of Langmuir, except that an allowance is made in the former for the surface binding vibrations of an adsorbed species. This model is given by:

$$.Q_e = Q_m(1 - e^{K_J C_e}) \quad (15)$$

where K_J and Q_m are the model constants. The linear form of equation (12) is given by equation (10):

$$lnQ_e = lnQ_m - K_J C_e \quad (16)$$

The plot of lnQ_e versus allows the determination of different constant [29,30].

2.4.13 Elovich isotherm model

The Elovich model is given by:

$$\frac{Q_E}{Q_m} = K_E C_e \exp\left(-\frac{Q_e}{Q_m}\right) \quad (17)$$

where K_E is Elovich constant [31].

The linearization of equation (11) is given by:

$$\ln\left(\frac{Q_e}{C_e}\right) = \ln(K_E Q_m) - \frac{Q_e}{Q_m} \quad (18)$$

The plot of $\ln\left(\frac{Q_e}{Q_m}\right)$ versus Q_e gives a straight line that can be used to determine the model constants [31].

2.4.14 Kiselev isotherm model

This model defined by Kiselev in 1948 is based on a monolayer adsorption and is given by:

$$K_1 C = \frac{\theta}{(1-\theta)(1+\theta K_n)} \quad (19)$$

Where K_1 is the equilibrium constant relative to adsorbate-adsorbent interaction, K_n is the constant of formation of complexes between adsorbed molecules and θ is the coverage surface (θ = Q_e/Q_m). Q_m is the maximum adsorbed quantities and it is obtained from the Langmuir model. The linear form is given by:

$$\frac{1}{(1-\theta)C_e} = \frac{K_1}{\theta} + K_1 K_n \quad (20)$$

The plot of $\frac{1}{(1-\theta)C_e}$ versus $\frac{1}{\theta}$ allows one to determine the different constants in the model [32].

3. RESULTS AND DISCUSSION

3.1 Characterization of Activated Carbons

3.1.1 SEM analysis

The morphological structures on the carbons were analyzed with the aid of SEM. The surface structures of the activated carbons have burnt out pores as shown in Fig. 1. Sample B,

activated carbon from ayous saw dust activated with 1 M H_3PO_4 (B1M) shows pore with tunnels or honeycomb-like structures. The SEM photographs for samples A, activated carbon from *Cucurbitaceae* peelings activated with 1 M H_3PO_4 (P1M) is characterized by a smooth surface with many orderly developed pores, compared to the others. Sample C, the mixture of *ayous* sawdust and *Cucurbitaceae* peelings activated with 1 M H_3PO_4 (BP1M) reduces the orderly pores development on the surface of the activated carbons. This can be a result of impurities such as tar produced by a*yous* sawdust in the mixture that could clog the pores and inhibit good pore structure development since the amount of activating agent stays constant during the production process. On the other hand, the well-developed pore form observed for B1M and P1M can be attributed to H_3PO_4 which hydrolyzes glycosidic linkages in the lignocellulosic materials and cleaves the aryl ether bonds in lignin. These reactions are accompanied by further chemical reactions that include dehydration, degradation and aromatic condensation [32]. This condensation forms linkages that retain carbon [33]. The linkage formation is probably responsible for this pore formation.

3.1.2 EDX analysis

EDX analysis indicates the presence of carbon, oxygen, phosphorous, potassium and chloride on surfaces of B1M and BP1M while in P1M we have just carbon and oxygen. The difference between the atoms present in each activated carbon can be attributed to the initial composition of ayous sawdust and cucurbitaceae peelings. The presence of phosphorous atom indicates that during the activated process, phosphate of H_3PO_4 reacted with ayous sawdust. Furthermore, in Fig. 2, the EDX analysis indicates a constant in the number of atoms in BP1M and B1M. This can be explained by the fact that during the analysis, the small amount of BP1M taken was constituted only by B1M. The presence of phosphorous atom confirms the pores development in B1M and BP1M compared to P1M. We can also see that in the mixture there is a transfer of the atom present in activated carbon obtained from each starting material. This can be attributed to the fact that, the reaction between H_3PO_4 and the different precursors still have the same as in individual precursors and since the temperature stay constant the atoms present in each individual activated carbon was transferred to the one obtained by mixing the precursors.

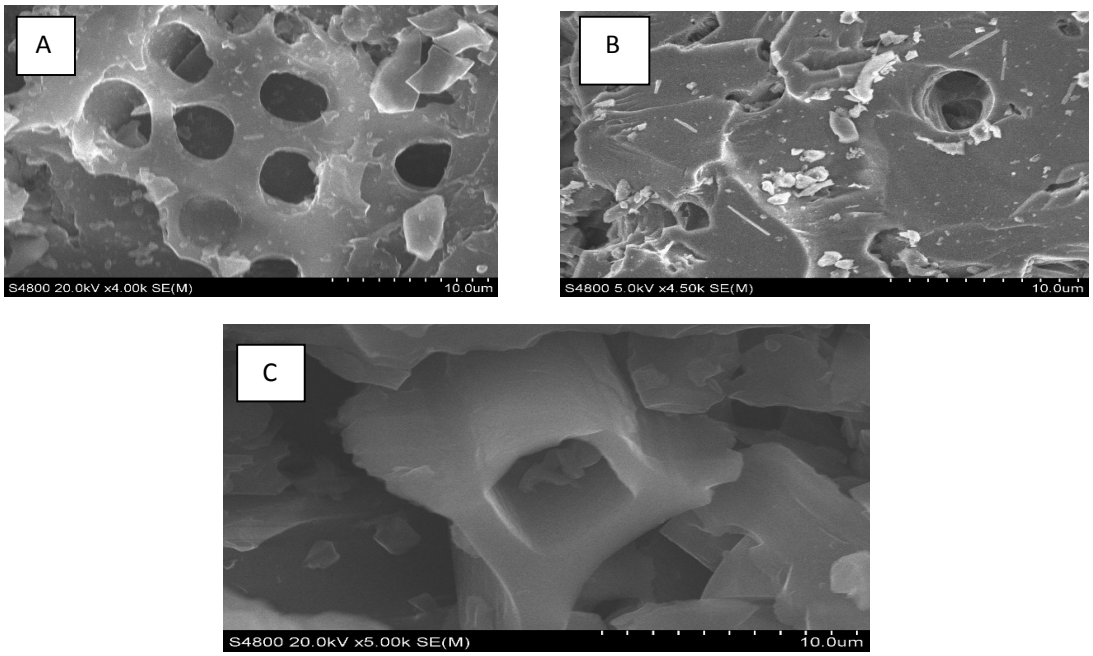

Fig. 1. The SEM photograph of the prepared activated carbons (A: B1M, B: P1M and C: BP1M)

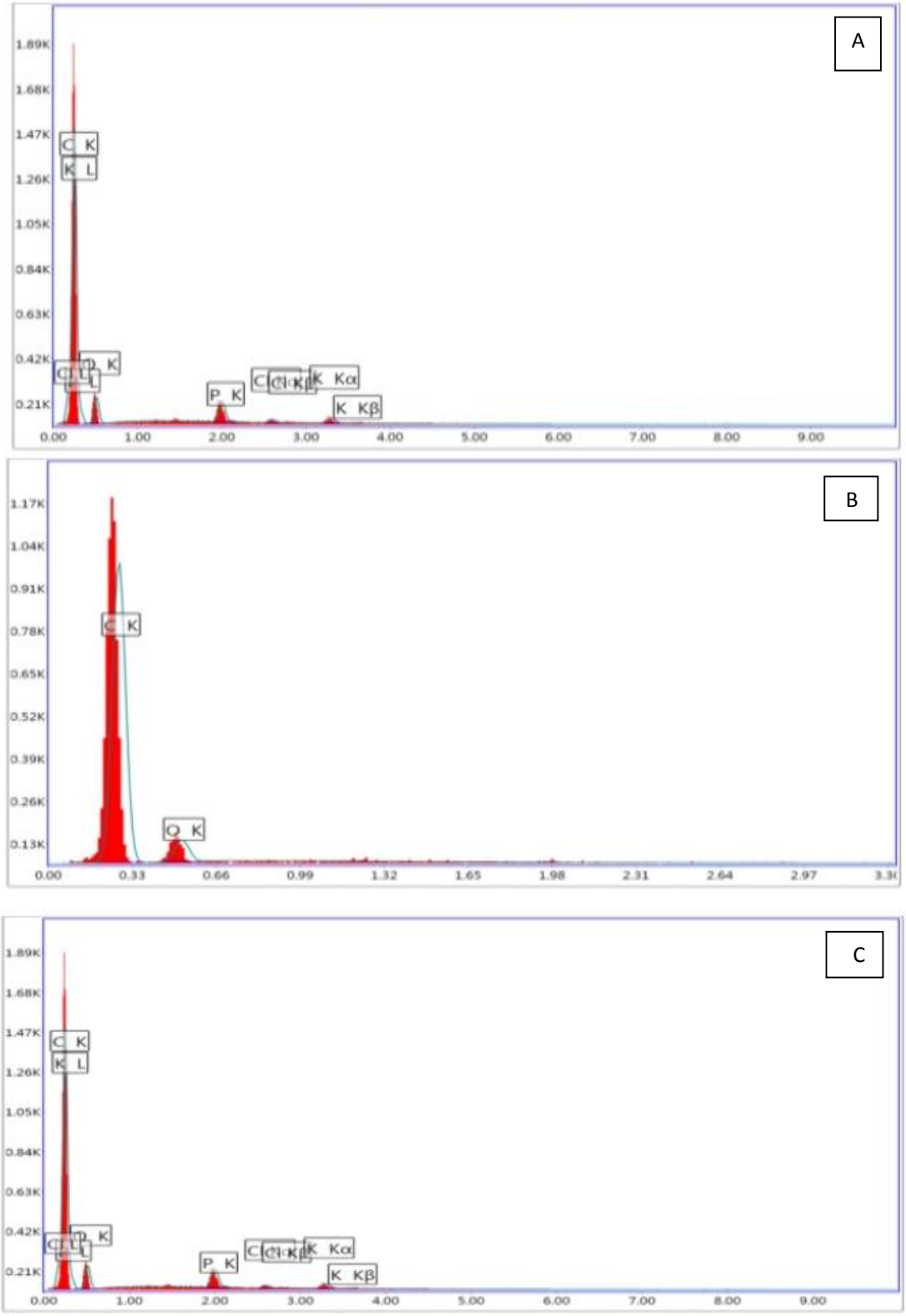

Fig. 2. EDX analysis of the prepared activated carbons (A: B1M, B: P1M and C: BP1M)

The percentage of the element present in the different activated carbons is given in Table 1.

3.1.3 FT-IR spectrum

The FT-IR spectroscopy was used to determine the various functional groups present in adsorbent materials. The spectrums obtained are shown in Fig. 3 below.

Comparing the adsorption peaks with those obtained for activated carbons, the following analyses can be obtained: 3300 cm^{-1}: -OH vibration of chelate and phenolic groups in the main constituents of lignocellulosic materials; 2860-2900 cm^{-1}: -CH_3, -CH- and -CH_2 vibration in cellulose, hemicelluloses and lignin; 1650-1740 cm^{-1}: -C=O vibration; 1260 cm^{-1}: –C-O vibration in carboxylic acids; 1050-1300 cm^{-1}: –C-O vibration in lactones; 900-600 cm^{-1}: vibration of aromatic polynuclear systems [34]. Fig. 3 also shows that all the spectra have the same peaks except one peak around 2200 cm^{-1} in the cases of the spectrum after adsorption. This and the larger peaks obtained after adsorption is proof that both activated carbons have adsorbed phenacetin. The similarity between the spectrum before and after adsorption in the case B1M is probably due to the small quantities adsorbed compare to the case of P1M and BP1M. In the case of BP1M the larger peaks near 1100 cm^{-1} after adsorption is probably due to the bonds form between phenacetin and BP1M.

3.2 Adsorption Study

3.2.1 Effect of initial pH

The pH of the solution influences the adsorption processes in that, it affects the surface charge of the adsorbent as well as the degree of ionization of the adsorbate [35]. The determination of pH point of zero charges (pH_{pzc}) for this activated carbon was carried out by adding 0.1 g of activated carbon to 40 mL solution of 0.1 M NaCl whose initial pH had been measured and adjusted with 0.1 M NaOH or 0.1 M HCl to vary between 3-11. The pH of zero point charge was also determined and the result was similar to those obtained by [16] and is given below.

The effect of the pH was studied in the pH interval 2 - 7 using an initial concentration of 40 mg/L for each adsorbent. The results obtained are presented in Fig. 4 below.

Table 1. Atomic percent of the elements present in the activated carbons

Elements	C (%)	O (%)	P (%)	Cl (%)	K (%)
B1M	85.38	12.82	1.17	0.19	0.44
P1M	92.81	7.19	/	/	/
BP1M	85.39	12.82	1.17	0.19	0.44

Where B1M is activated carbon from ayous sawdust, P1M is activated carbon from cucurbitaceae peelings and BP1M is activated carbon from the mixture of ayous sawdust and cucurbitaceae peelings

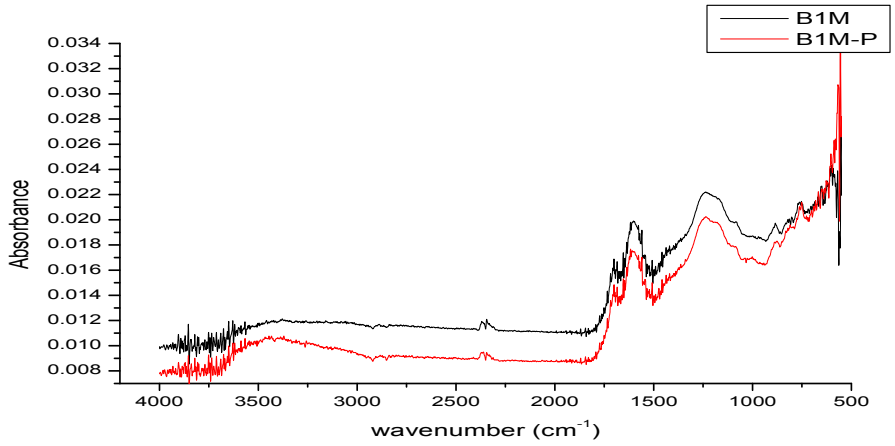

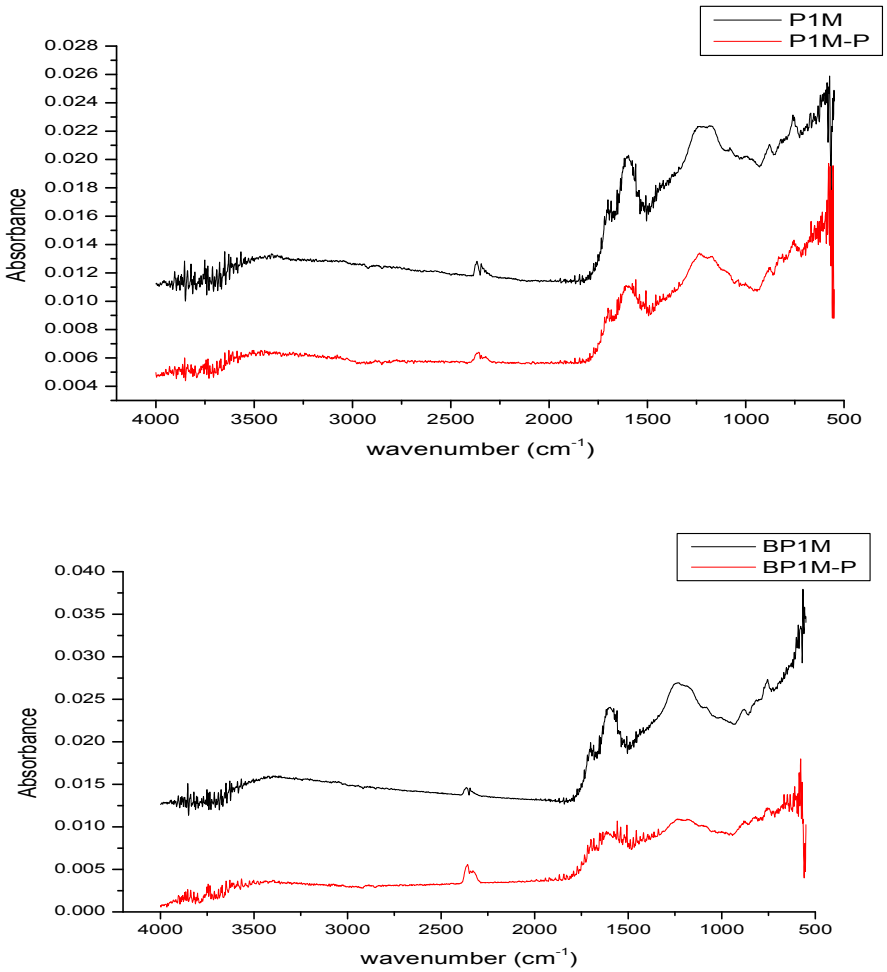

Fig. 3. FT-IR Spectra of activated carbon without adsorption (back) and after adsorption (Red)

The results show that adsorption is favoured for pH < $pH_{PZC,}$ where pH_{PZC} is the pH at the point of zero charges. Maximum adsorption was observed at a pH of 2. The pH_{PZC} obtained for the various carbons are 6.1 for B1M, 6.5 for P1M and 6.3 for BP1M [18]. The maximum adsorption at pH = 2, which is lower than the pH_{PZC} for the three carbons can be explained by the fact that, at this pH, the surface of the materials are positively charged. This charge can create an ionic exchange between the surface and the protonated amino functional group of phenacetin as shown below:

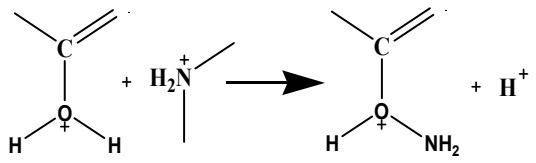

With pH > pH_{PZC}, the adsorbate is more soluble, and the negative charges of the surface of the activated carbons increase the electrostatic force of repulsion between adsorbate (amino functional group of phenacetin) and –OH groups of the surface of the material [36].

Table 2. pH of zero point charge of different activated carbons

Activated carbon	B1M	P1M	BP1M
pH_{zpc}	6.1	6.5	6.3

3.2.2 Effect of contact time

The time of agitation is a very significant parameter in the adsorption process, because it makes it possible to determine the time necessary to reach equilibrium adsorption,

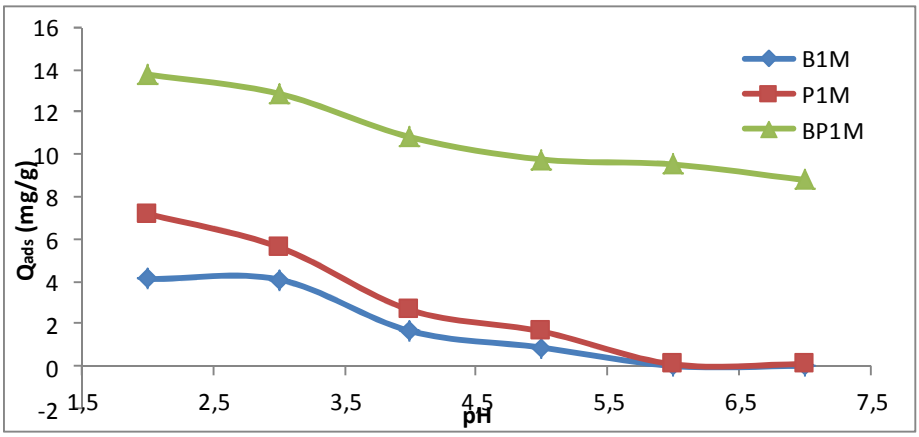

Fig. 4. Influence of pH on the adsorption of phenacetin

and also to study the kinetics of the adsorption process. Studies on the adsorption of phenacetin of initial concentration 40 mg/L in aqueous solution were carried out with 30 mL solution of adsorbate, and the results are presented in Fig. 5. The figures show the evolution of the capacity of adsorption of each compound with time at ambient temperature. The results show that the adsorption process takes place in two stages. The first stage was observed during the first 45 minutes of adsorption. The second stage was much slower and took a longer time. The occurrence of the fast phase can be explained by the fact that, at the start of the process all the sites on the adsorbent are available, and the phenacetin molecules readily occupy them. The same tendency had been obtained by [37]. The slow phase which ends at the onset of equilibrium occurs because the presence of the carboxylic and hydroxyl groups inhibits the adsorption of the organic compounds [38,39]. The adsorbed quantities can be attributed to π-π interactions. Indeed, during the aromatic condensation, it is possible that surface functional groups do not occupy the entire nucleophilic sites on the surface. During the adsorption process, these nucleophilic sites can react with the electrophilic ones on the benzene ring of phenacetin. The high quantities of phenacetin adsorbed by the mixture (13.18 mg/g for BP1M; 7.40 mg/g for P1M and 4.11 mg/g for B1M) can be attributed to the development of both types of pores. Also, the mixture of both precursors increases the percentage of cellulose which favours the development of microporosity, which is responsible for the adsorption of phenacetin [40].

The results also reveal that the time to achieve equilibrium adsorption is the same for all the different adsorbents. Thus, equilibrium for phenacetin was attained in 120 minutes. This implies that the kinetics of adsorption is not influenced by the mixture of starting materials used in preparing the activated carbon.

3.2.3 Ionic strength

Wastewater containing pharmaceuticals may also have higher salt concentration since many metals of group I and II are present in drugs, and the effects of ionic strength are also of importance in the study of the adsorption of pharmaceuticals onto adsorbents. Fig. 6 shows the effect of various concentrations of KCl, $CaCl_2$ and $MgCl_2$ on the efficiency activated carbons to adsorb phenacetin of initial concentration 40 mg/L. On this figure, it can be seen that the addition of salt does not affect the adsorption capacities for P1M but increase in the case of B1M and BP1M. Theoretically, when the electrostatic attraction is repulsive, an increase in ionic strength will increase adsorption [41-42]. The significant increase in phenacetin removal after salts addition by B1M and BP1M can be attributed to an increase in dimerization of phenacetin in solution [43]. A number of intermolecular forces have been suggested to explain this aggregation; these forces include van der Waals forces, ion-dipole forces, and dipole-dipole forces, which occur between phenacetin molecules in the solution. The higher adsorption capacity of phenacetin under these conditions can be attributed to the aggregation of molecules induced by the action of salt ions. That is, salt ions force phenacetin molecules to

aggregate, thereby increasing the extent of sorption on the surface of the activated carbon. [42,43] also reported an increase in the adsorption of reactive dye after adding salt to the solution.

The addition of calcium ions has a far greater effect than the addition of potassium and magnesium ions. This cannot be explained in terms of ionic strength alone, but it is also considered that the adsorbed calcium-phenacetin complex is more stable than the magnesium-phenacetin and potassium-phenacetin complexes [44,45].

The effect of the salts on contact time was also investigated and the results obtained are given in the Fig. 6. It can be seen that these curves have the same shape as those of contact time. This can be a proof that adsorption mechanism does not change when we add salts; even those of group I or group II elements to the adsorbate solution. The increase in adsorbed quantity can also be attributed to the reduction of solubility of phenacetin by the salt [37,46].

3.2.4 Kinetic study

The kinetic models used to investigate and describe the adsorption of phenacetin are pseudo-first order, pseudo-second order, and Elovich models. The plots of the kinetic models are presented in Fig. 8. The validity of the order of adsorption process is based on the regression coefficients, R^2 and on the predicted values of Q_e. The parameters for the kinetics models are presented in Table 3.

As seen from Table 3, it is evident that the adsorption of phenacetin onto the activated carbons adequately follows the pseudo-second-order kinetic model, as the correlation coefficients are higher than 0.9 for both adsorbents, and the predicted maximum adsorbed quantities are close to the experimental value of 4.11 mg/g for B1M, 7.40 mg/g for P1M and 13.11 mg/g for BP1M. This allows us to conclude that the rate-limiting step is chemisorption. This involves interactions caused by sharing of π electrons or exchange of protons in a high acid milieu (pH= 2) between sorbent and sorbate [47].

Pseudo-first order kinetic model is in agreement with a multi-layer adsorption on the surfaces. According to the correlation coefficient, phenacetin adsorption in the case of B1M is multi-layer. This can explain the lower value of adsorbed quantities obtained. Indeed, the physical bond is weak and can be easily broken during adsorption and therefore reduce the adsorbed quantities. We can also see in Table 3 that the presence of salt favor multi-layer adsorption.

3.2.5 Adsorption mechanism

The mechanism of adsorption is generally considered to involve three steps, one or any combination of which can be the rate-controlling mechanism. These steps are:

(i) Mass transfer across the external liquid film surrounding the particle;
(ii) Adsorption at a site on the internal or external surface of the adsorbent; and the energy will depend on the binding process: whether physical or chemical.
(iii) Diffusion of the adsorbate molecules to an adsorption site either by a pore diffusion process through the liquid film process or by a solid surface diffusion mechanism.

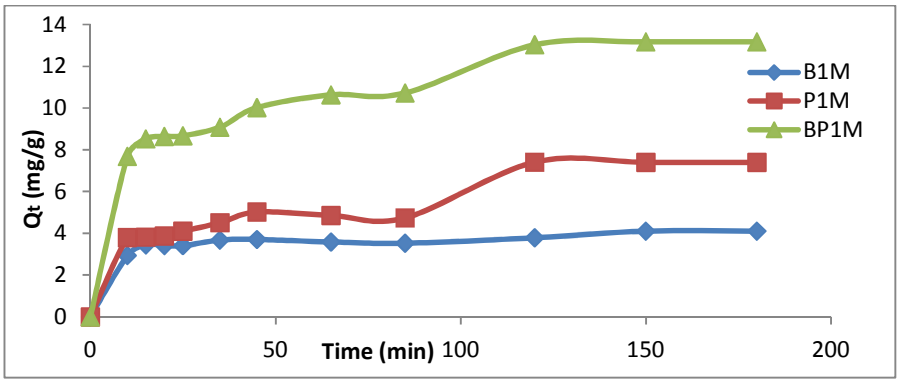

Fig. 5. Effect of contact time on phenacetin adsorption by the activated carbons

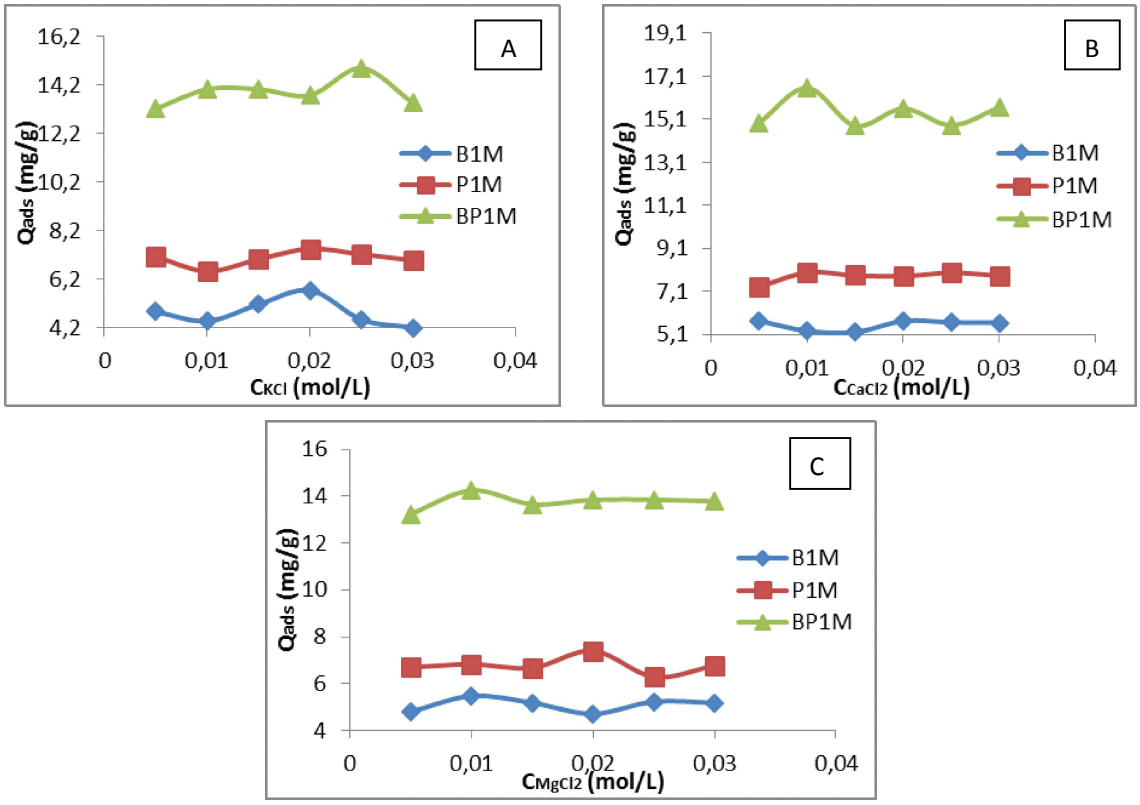

Fig. 6. Effect of initial concentration of salt on the adsorbed quantities (A: effect of KCl, B: effect of $CaCl_2$ and C: effect of $MgCl_2$)

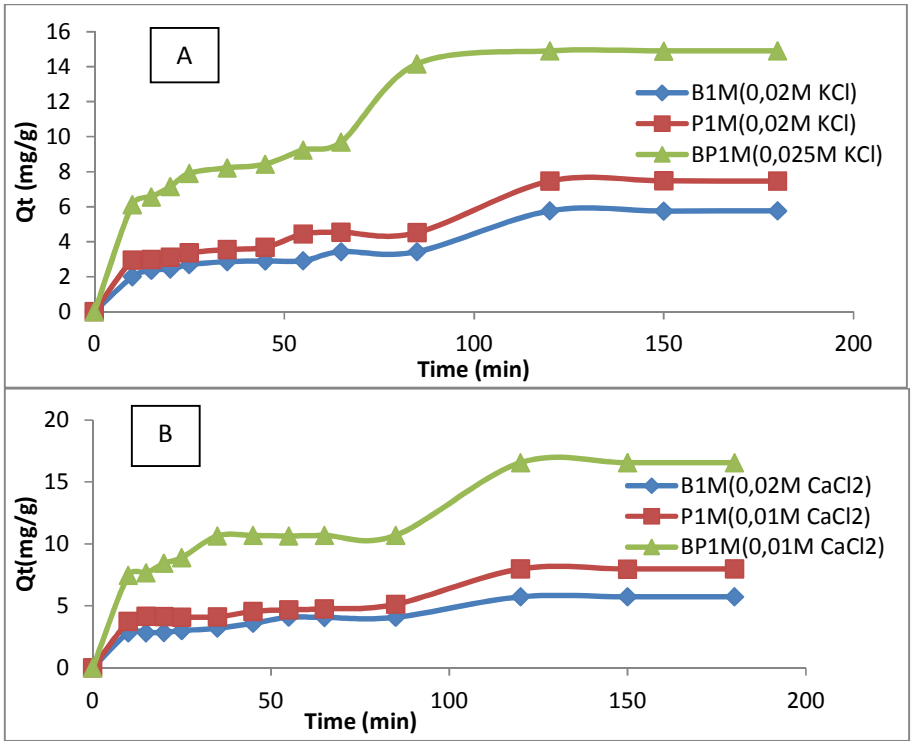

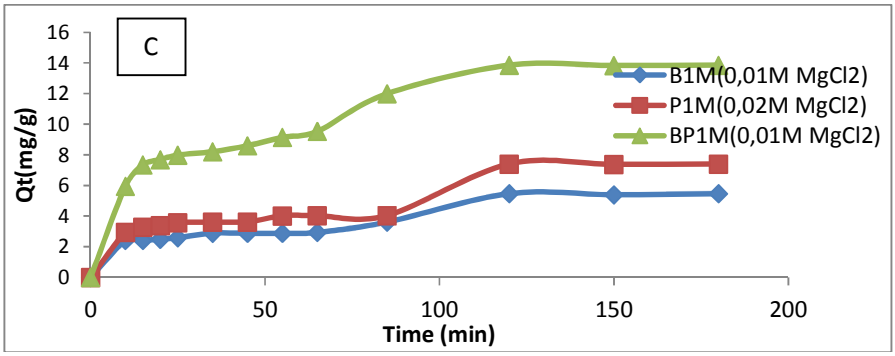

Fig. 7. Effect of salts on the contact time (A: effect of KCl, B: effect of $CaCl_2$ and C: effect of $MgCl_2$)

From the plots of Q_t versus $t^{0.5}$ multi-linearity was observed for BP1M and one linearity for B1M and P1M. Multi-linearity, implying that more than one mechanism affected the adsorption process. The first portion describes the gradual adsorption stage or external mass transfer effects. These lines do not pass through the origin, indicating that the intraparticle diffusion is not the only process that can control the kinetics of adsorption. The second portion (case of BP1M) is attributed to the final equilibrium stage for which the intraparticle diffusion started to slow down due to the extremely low amount of phenacetin compounds left in the solution. We can see in Table 4 that the presence of salts favors diffusion of phenacetin into activated carbon adsorption site by reducing the boundary layer thickness. In the case of BP1M the two phases observe can be the result of the mixture of the precursors. Indeed, SEM analysis shows that P1M have in majority meso-pores who can favors mass transfer across the external liquid film surrounding and B1M have micro-pore who can be considered as the site of adsorption. This explanation can also be related to the boundary layer thickness constant (C) who is high in the first linearity and low in the second linearity.

In order to study the effect of different salts on the initial rate of adsorption (h_o) given by the pseudo-second-order model and the desorption rate constant (β) given by the Elovich model, the histograms presented in Fig. 8 were plotted. On the figure, it is seen that addition of $CaCl_2$ increases the initial rate of adsorption for P1M, BP1M more than the other salts and it reduces more the rate of desorption. This can be attributed to the high molecular weight of $CaCl_2$ which reduces the solubility and favours adsorption [36]. The value of the desorption rate constant confirms the low quantities adsorbed by B1M. Based on the rate constant, we can say that the bond established between B1M and phenacetin is a low energy band corresponding to the highest value of the constant, while the bond energy in P1M and BP1M is high which corresponds to the lowest value of the constant, since desorption is favorable in physisorption than in chemisorption.

3.3 Equilibrium Study

To study the equilibrium, the initial concentration of adsorbate was varied, while maintaining constant the other parameters such as pH, the volume of the solution, time of contact and the mass of adsorbent. When the initial concentration was increased from 20 to 50 mg/L, the capacity of adsorption for the three carbons was observed to increase (Fig. 9). This increase in the capacities of adsorption for the activated carbons with the increase in the concentration of phenacetin can be attributed to π–π interactions and the exchange of protons between these organic compounds and the functional groups on the carbon surface. The same result was obtained by [37]. The π-π interactions in most cases are responsible for the mechanism of adsorption of aromatic compound [48-50].

The Langmuir, Freundlich, Jovanovic, Kiselev, Elovich models were studied in this work. The adsorption isotherms relate the amount of phenacetin adsorbed at equilibrium Qe (mg/g) to the phenacetin concentration at equilibrium, Ce (mg/L) and the plots are given in Figs. 10 to 14.

Table 3. Parameters of kinetics models for phenacetin adsorption on B1M, P1M and BP1M

Model	Pseudo-second order				Elovich models			Pseudo-first order		
Parameters	**Q_e (mg/g)**	**h_o (mg/g.min)**	**K_2 (g/min.mg)**	**R^2**	**α (mg/g.min)**	**β (mg/g.min)**	**R^2**	**K_1 (1/min)**	**Qe (mg/g)**	**R^2**
B1M	4.15	0.69	0.004	0.994	963.25	3.24	0.669	0.0074	1.246	0.780
P1M	8.24	0.31	0.0046	0.935	11.36	1.4	0.832	0.0052	3.671	0.660
BP1M	14.18	0.92	0.0045	0.990	26.19	0.67	0.927	0.027	9.325	0.780
B1M + KCl	3.77	0.36	0.025	0.986	1.58	1.58	0.917	0.0061	3.746	0.903
P1M+ KCl	5.15	0.43	0.016	0.981	1.84	1.14	0.856	0.0069	4.893	0.905
BP1M+KCl	14.75	0.64	0.003	0.859	4.47	0.53	0.917	0.024	14.35	0.677
B1M+$CaCl_2$	4.62	0.42	0.02	0.985	2.26	1.35	0.867	0.0096	3.325	0.890
P1M+$CaCl_2$	5.31	0.83	0.03	0.991	43.12	1.78	0.857	0.0047	4.317	0.931
BP1M+$CaCl_2$	11.72	1.84	0.013	0.995	10.08	0.54	0.878	0.0065	8.930	0.712
B1M+$MgCl_2$	3.63	0.40	0.03	0.967	5.89	2.15	0.780	0.0057	3.325	0.855
P1M+$MgCl_2$	5.31	0.81	0.028	0.996	20	1.98	0.934	0.0036	4.342	0.851
BP1M+$MgCl_2$	12.51	0.85	0.0038	0.950	3.41	0.46	0.850	0.015	9.121	0.838

Where B1M is activated carbon from ayous sawdust, P1M is activated carbon from cucurbitaceae peelings and BP1M is activated carbon from the mixture of ayous sawdust and cucurbitaceae peelings

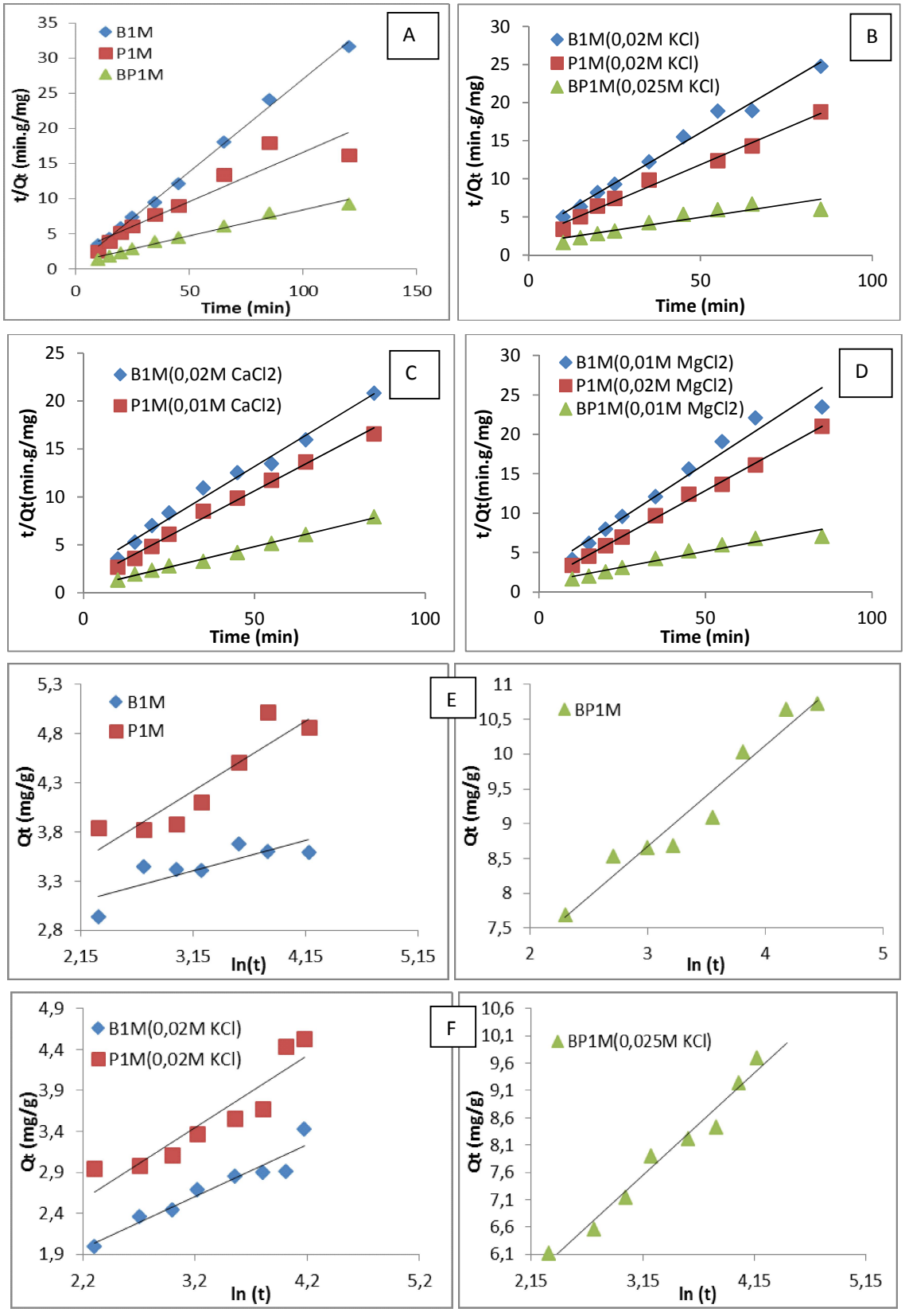
A
B1M
P1M
BP1M
t/Qt (min.g/mg)
Time (min)
B
B1M(0,02M KCl)
P1M(0,02M KCl)
BP1M(0,025M KCl)
t/Qt (min.g/mg)
Time (min)
C
B1M(0,02M CaCl2)
P1M(0,01M CaCl2)
t/Qt(min.g/mg)
Time (min)
D
B1M(0,01M MgCl2)
P1M(0,02M MgCl2)
BP1M(0,01M MgCl2)
t/Qt(min.g/mg)
Time (min)
E
B1M
P1M
Qt (mg/g)
ln(t)
BP1M
Qt (mg/g)
ln (t)
F
B1M(0,02M KCl)
P1M(0,02M KCl)
Qt (mg/g)
ln (t)
BP1M(0,025M KCl)
Qt (mg/g)
ln (t)

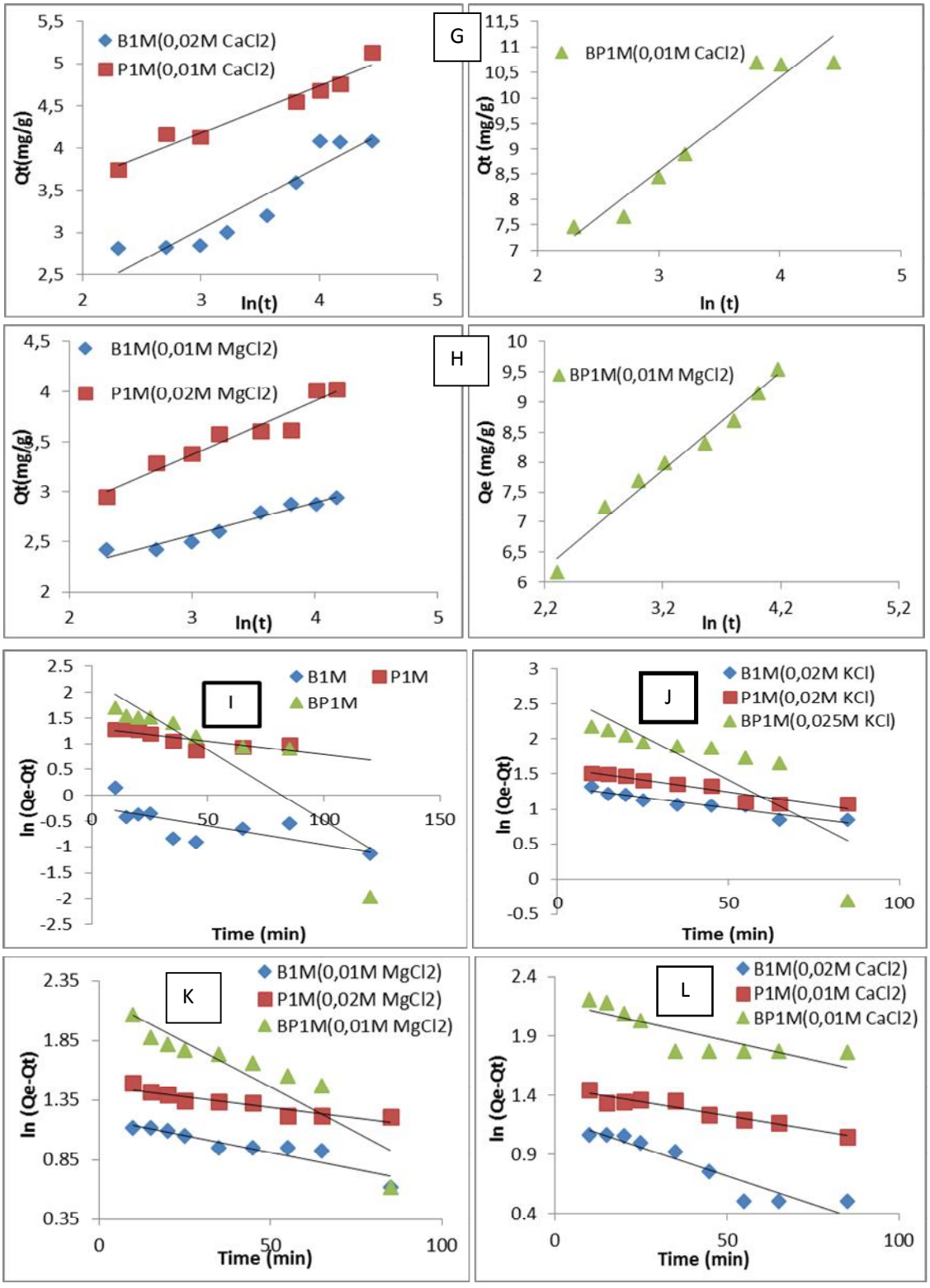

Fig. 8. Linearized pseudo-second order (A: no sel, B: with KCl, C: with $CaCl_2$, D: with $MgCl_2$), Elovich (E: no sel, F: with KCl, G: with $CaCl_2$, H: with $MgCl_2$), pseudo-first order (I: no sel, J: with KCl, K: with $CaCl_2$, L: with $MgCl_2$) plots

The different constants derived from the graphs of the models are grouped in Table 4.

According to the R^2 values presented in Table 4 we can conclude that the adsorption process adequately follows the Langmuir isotherm model which is based on the assumption that uptake occurs on a homogenous surface by monolayer sorption without interaction between adsorbed molecules. The R_L values from the Langmuir model range between 0 and 1 implying that the adsorption of phenacetin is favorable. The Freundlich sorption isotherm shows that adsorption is favorable for P1M and BP1M because then value ranges between 1 and 10 and unfavorable for B1M, where n is higher than 10 [32]. From the Jovanovic isotherm model it can be concluded that adsorption is a monolayer localized process, which does have lateral interactions; just like in the case of the Langmuir model [30]. The Kiselev isotherm model shows that there is no formation of a complex between the adsorbate molecules during adsorption since all of the constants are negative [33].

Table 4. Constants of Weber and Morris diffusion model

Activated carbon	Constants	Without salts	KCl	$MgCl_2$	$CaCl_2$
B1M	K_{id} (mg/g.min)	0.058	0.224	0.204	0.256
	C (mg/g)	3.224	1.438	1.640	1.801
	R^2	0.786	0.982	0.951	0.907
P1M	K_{id} (mg/g.min)	0.234	0.311	0.169	0.203
	C (mg/g)	2.985	1.817	2.594	3.164
	R^2	0.847	0.959	0.822	0.905
BP1M (1): first linearity	K_{id} (mg/g.min)	0.448	0.822	0.756	0.816
	C (mg/g)	6.518	3.507	4.009	4.749
	R^2	0.843	0.959	0.822	0.937
BP1M (2): second linearity	K_{id} (mg/g.min)	0.679	2.369	1.350	1.052
	C (mg/g)	5.174	-7.826	-0.783	2.886
	R^2	0.853	0.978	0.920	0.918

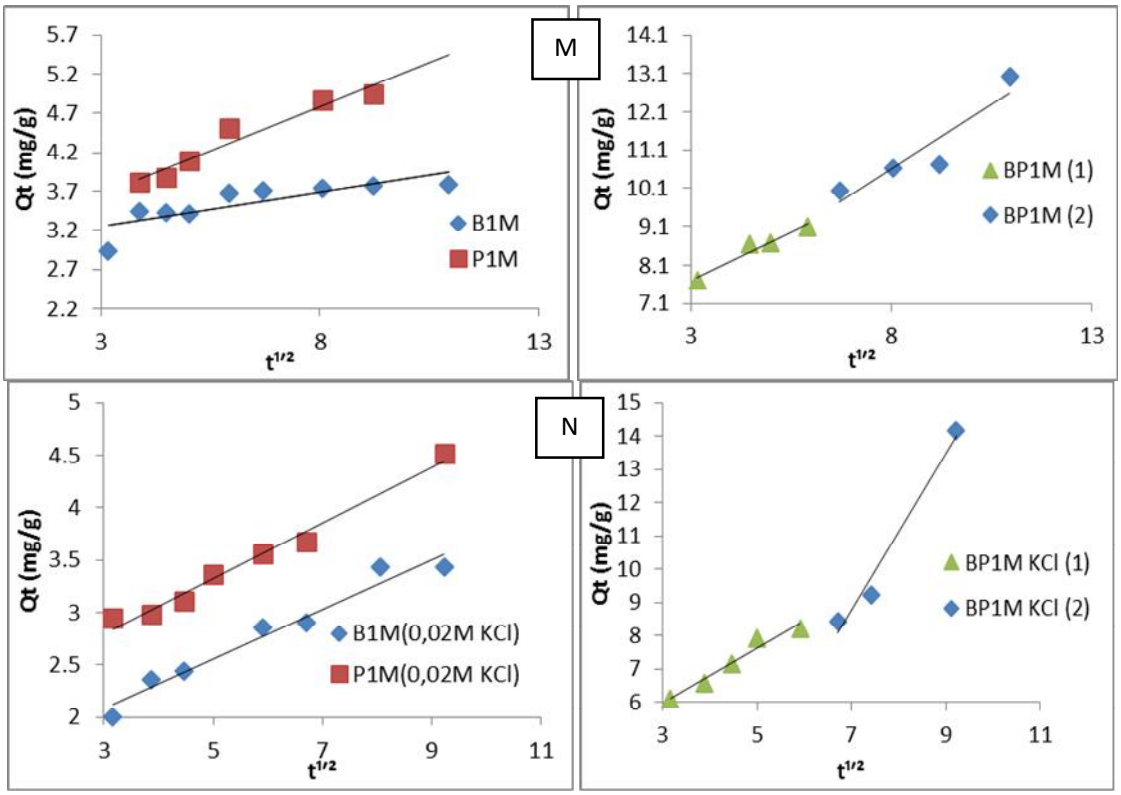

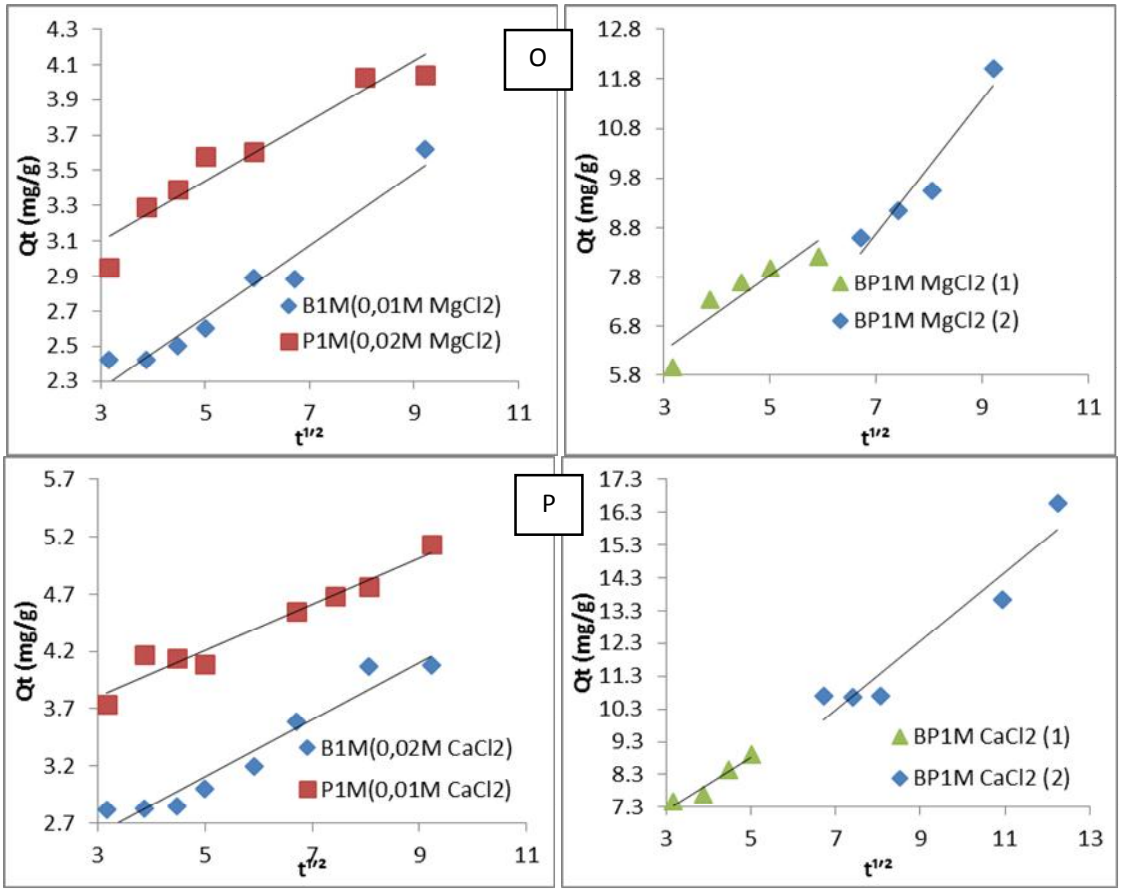

Fig. 9. Weber & Morris intraparticle diffusion (M: no sel, N: with KCl, O: with $CaCl_2$, P: with $MgCl_2$) plots

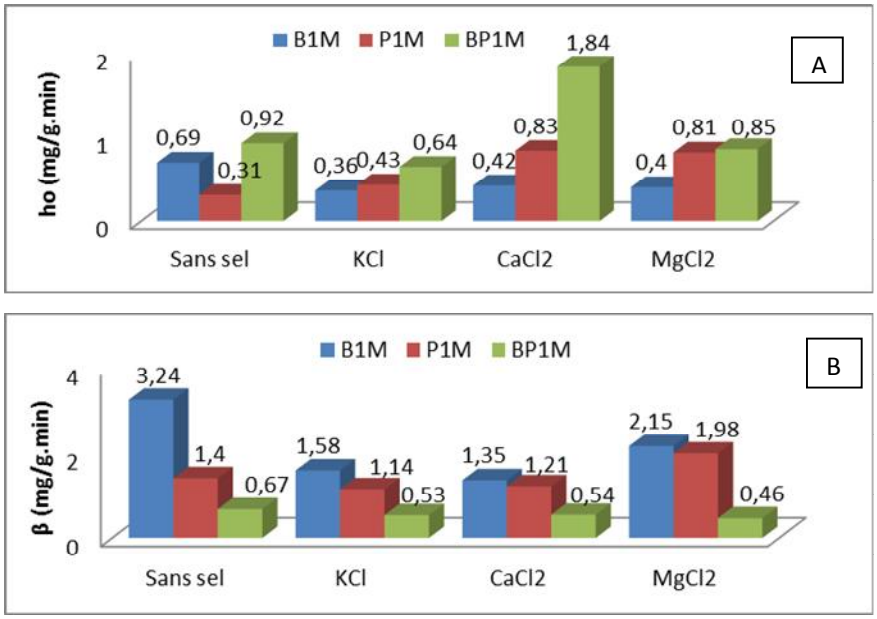

Fig. 10. Effect of different salts on the initial rate of adsorption (A) and the desorption rate constant (B)

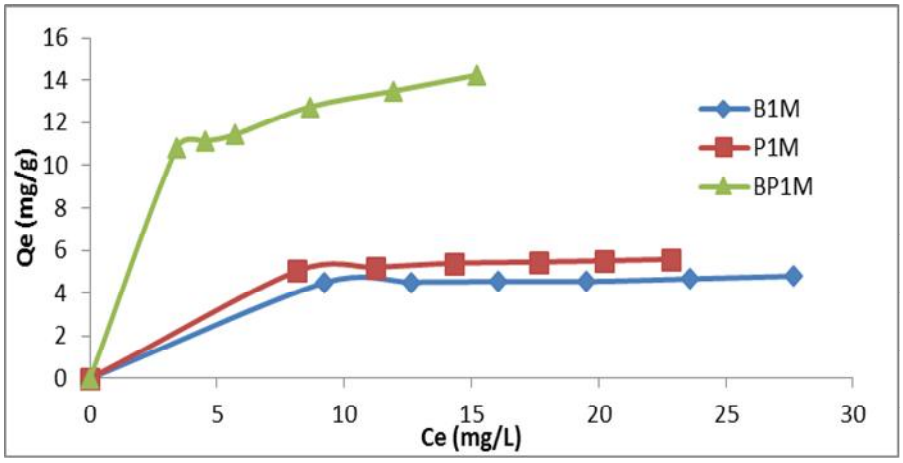

Fig. 11. Effect of initial concentration on adsorbed quantities

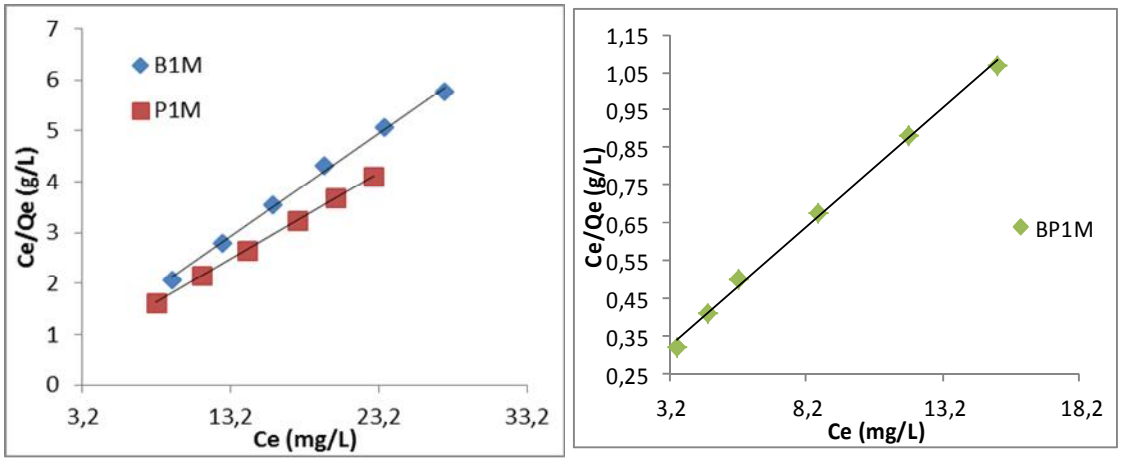

Fig. 12. Linear transformation of Langmuir model

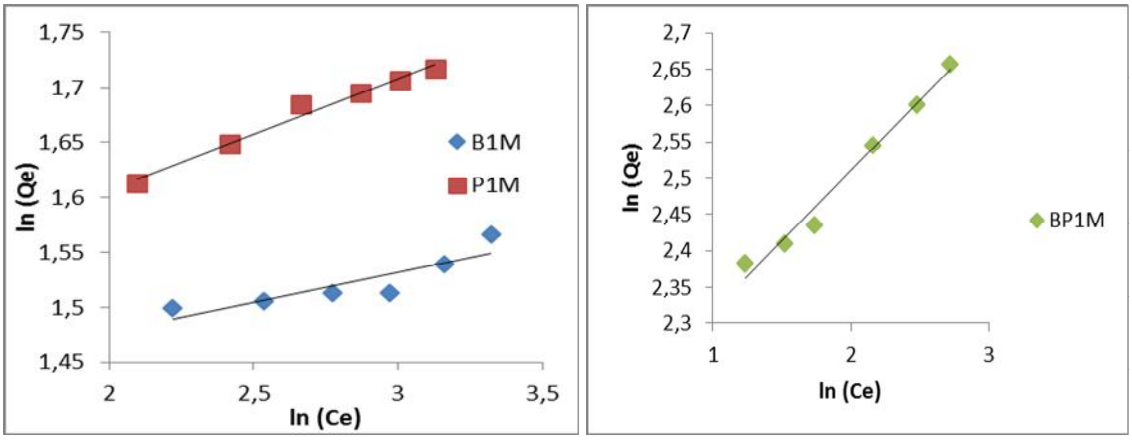

Fig. 13. Linear transformation of Freundlich model

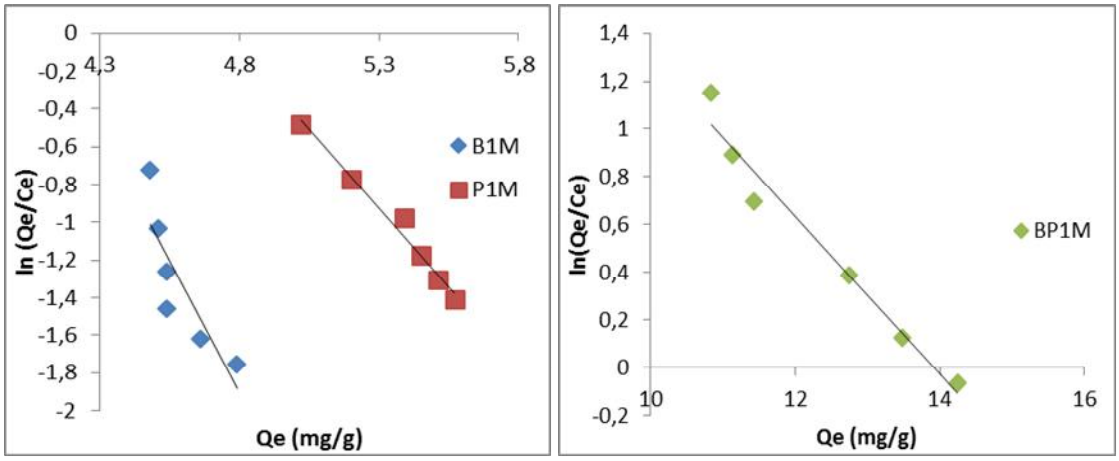

Fig. 14. Linear transformation of Elovich model

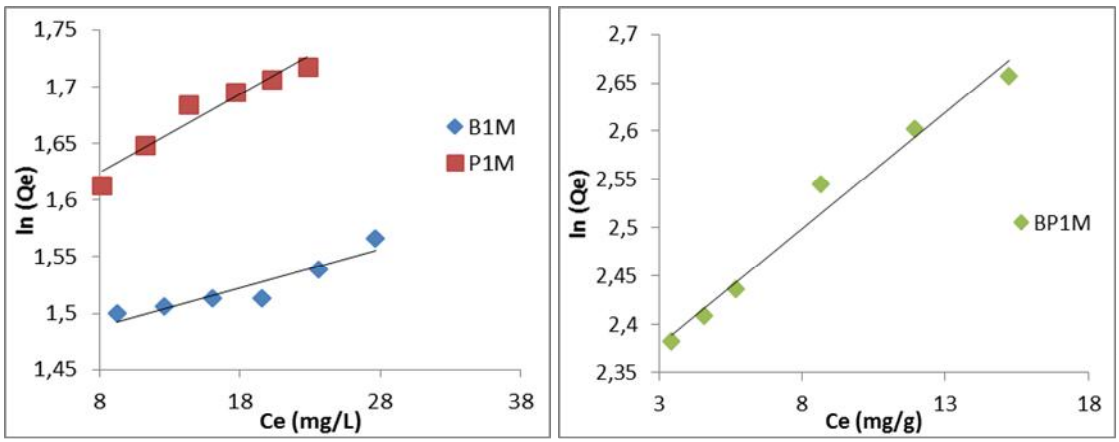

Fig. 15. Linear transformation of the Jovanovic model

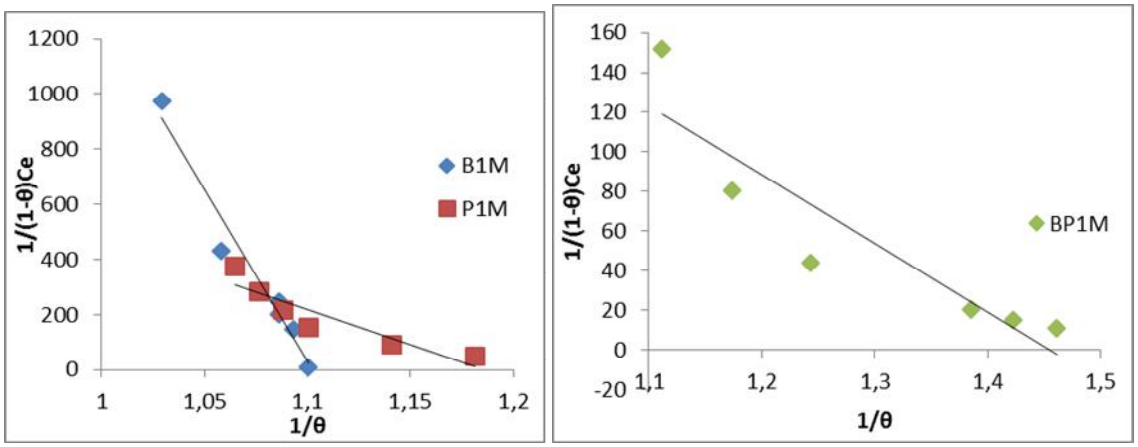

Fig. 16. Linear transformation of the Kiselev model

Table 5. Constants of Isotherm models

Models	Constants	B1M	P1M	BP1M
Langmuir	K_L (L/mg)	0.82	0.66	0.52
	Q_m (mg/g)	4.93	5.93	15.84
	R_L	0.026	0.032	0.04
	R^2	0.997	0.999	0.997
Freundlich	K_F (mg/L)	3.93	4.08	8.38
	1/n	0.054	0.168	0.063
	R^2	0.763	0.981	0.982
Jovanovic	K_J (L/mg)	0.0034	0.0068	0.0241
	Q_m (mg/g)	4.31	4.81	10.04
	R^2	0.870	0.931	0.978
Elovich	K_E (L/mg)	3.18×10^{5}	4.33×10^{3}	32.45
	Q_m (mg/g)	0.35	0.6	3.03
	R^2	0.730	0.980	0.966
Kiselev	K_1 (L/mg)	-1.18×10^{4}	-2.52×10^{3}	-3.47×10^{2}
	Kn	-1.10	-1.19	-1.45
	R^2	0.952	0.843	0.837

4. CONCLUSION

Activated carbons produced from *ayous* sawdust and c*ucurbitaceae* peelings were successfully utilized for the removal of phenacetin from aqueous solution by batch adsorption method. Characterization showed that in the activated carbon obtained from the mixture of precursor materials, there was a transfer of atoms present in each activated carbon separately. On the result of the SEM analysis, we can see that the mixture has standardized the varieties of pores observed in the case of P1M. FT-IR analysis shows that after adsorption one peak around 2200 cm^{-1}. This is the proof that both activated carbons have adsorbed phenacetin and the larger peaks near 1100 cm^{-1} after adsorption is probably due to the bonds form between phenacetin and activated carbons. Adsorption is found to favorable at pH 2 because of electrostatic interactions. One of the important results obtained was the increase of quantities adsorbed by the mixture of the precursors who can be attributed to the standardization of pores obtained. The equilibrium data were tested using the Langmuir, Freundlich, Elovich, Jovanovic and Kiselev models. Correlation coefficient shows that Langmuir model described well the adsorption process. Kinetic parameters were also analyzed using the pseudo-second-order, and Elovich models. Kinetics studies showed that the adsorption followed pseudo-second-order. Ionic strength study shows that $CaCl_2$ increased the adsorbed quantities while $MgCl_2$ increased the rate constant of desorption. Multi-linearity observed in Weber and Morris diffusion model, implying that more than one mechanism affected the adsorption process. The first portion describes the gradual adsorption stage or external mass transfer effects. These lines do not pass through the origin, indicating that the intraparticle diffusion is not the only process that can control the kinetics of adsorption. We have also found that the mixture of the precursors favor the mass transfer from the solution to the adsorption site inside the activated carbons. Based on the fact that the mixture of precursors in the preparation of activated carbon increased the adsorbed quantities, this way of preparation must be explored because it can allow the user of some precursors who show poor adsorption capacities when they are used own.

ACKNOWLEDGEMENTS

Technical assistance rendered by the researchers of LANOCHEE Laboratory of the Department of Chemistry, University of Dschang (Cameroon) is gratefully acknowledged.

COMPETING INTERESTS

Authors have declared that no competing interests exist.

REFERENCES

1. Kolpin DW, Furlong ET, Meyer M, Thurman EM, Zaugg SD, Barber LB, Buxton HAT. Pharmaceuticals, hormones and other organic wastewater contaminants in US streams, 1999-2000: A national reconnaissance. Environmental

Science and Technology. 2002;36:1202-1211.
2. Ternes TA. Occurrence of drugs in German sewage treatment plants and rivers. Water Research. 1998;32:3245-3260.
3. Zawilska BJ, Wojcieszak J, Olejniczak BA. Prodrugs: A challenge for the drug development. Pharmacological Report. 2013;65:1–14.
4. Hinson JA. Reactive metabolites of phenacetin and acetaminophen: A review. Environmental Health Perspectives. 1983; 49:71-79.
5. Zuccato E, Calamari D, Natangelo M, Fanelli R. Presence of therapeutic drugs in the environment. The Lancet. 2000;355: 1789-1790.
6. Anwar El-S, Nagwa A. El-M, El-Hawary HH. Averting cancer effect of paracetamol and phenacetin by N-Acetylcystine. International Journal of Pharmacy and Pharmaceutical Sciences. 2014;6(5):383-390.
7. Brune K, Renner B, Tiegs G. Acetaminophen/paracetamol: A history of errors, failures and false decisions. European Journal of Pain. 2014;13. DOI: 10.1002/ejp.621;
8. Essomba JS, Ndi JN, Belibi BPD, Tagne GM, Ketcha JM. Adsorption of cadmium (II) ions from aqueous solution onto kaolinite and metakaolinite. Pure and Applied Chemical Sciences. 2014;2(1):11–30.
9. Abdellah A, Abdelkader I, Mohand SO. Hg (II) sorption from aqueous solution by blast-furnace slag. Water Quality Research Journal of Canada. 2007;42(1):41-45.
10. Akporhonor EE, Egwaikhide PA. Removal of selected metal ions from aqueous solution by adsorption onto chemically modified maize cobs. Scientific Research and Essay. 2007;2(4):132-134.
11. Vieira RSHF, Boya V. Biosorption: A solution to pollution. International Microbiology. 2002;3:17-24.
12. Mohammed-Khah A, Ansari R. Activated charcoal: Preparation, characterization and applications: A review article. International Journal of ChemTech Research. 2009; 1(4):859-864.
13. Taer E, Deraman M, Talib IA, Awitdrus A, Hashmi SA, Umar AA. Preparation of a highly porous binderless activated carbon monolith from rubber wood sawdustby a multi-step activation process for application in supercapacitors. International Journal of Electrochemical Science. 2011;6:3301-3315.
14. Kakoi B, Kaluli WJ, Thumbi G, Gachanja A. Performance of activated carbon prepared from sawdust as an adsorbent for endosulfan pesticide. Journal of Suitanable Research in Engineering. 2015;2(1):1-10.
15. Huang Y, Ma E, Zhao G. Optimization of the pore structure of bio-based ACFs through a simple KOH-steam reactivation. Materials. 2016;9:432.
16. MINADER, Annuaire des statistiques du secteur agricole. Campagne 2007- 2008. AGRI-STAT Cameroun, n°16, février. 2010;98.
17. Cerutti PO, Mbongo M, Vandenhaute M. Etat du secteur forêts-bois du Cameroun (2015). Publié par Organisation des Nations Unies pour l'alimentation et l'agriculture et Centre de recherche forestière internationale (CIFOR). 2016;42.
18. Ngakou SC, Ngomo HM, Tchuifon TDR, Anagho SG. Optimisation of activated carbon preparation by chemical activation of ayous sawdust, curcurbitaceae peelings and hen egg shells using response surface methodology. International Research Journal of Pure & Applied Chemistry. 2017;14(4):1-12.
19. Khavryuchenko DV, Khavryuchenko VO, Shkilnyy IA, Stratiichuk DA, Lisnyak VV. Characterization by SEM, TEM and quantum-chemical simulations of the spherical carbon with nitrogen (SCN) active carbon produced by thermal decomposition of Poly(vinylpyridine-divinylbenzene) Copolymer. Materials. 2009;2:1239-1251.
20. Abechi SE, Gimba CE, Uzairu A, Dallatu YA. Preparation and characterization of activated carbon from palm kernel shell by chemical activation. Research Journal of Chemical Sciences. 2013;3(7):54-61.
21. Ho YS, Ofomaja AE. Kinetic studies of copper ion adsorption on palm kernel fibre. Journal of Hazardous Materials. 2006; 137:1796–1802.
22. Ho YS, McKay G. Application of Kinetic Models to the Sorption of Copper(II) on to Peat. Adsorption Science and Technology. 2002;20(8):797-815.
23. Anagho SG, Ketcha JM, Tchuifon TDR, Ndi JN. Kinetic and equilibrium studies of the adsorption of mercury (II) ions from aqueous solution using kaolinite and metakaolinite clays from Southern

Cameroon. International Journal of Research in Chemistry and Environment. 2013;3:1-11.
24. Elovich SY, Larinov OG. Theory of Adsorption from Solutions of non-electrolytes on solid (I) equation adsorption from solutions and the analysis of its simplest form (II), verification of the equation of adsorption isotherm from solutions. Izv. Akad. Nauk. SSSR, Otd. Khim. Nauk. 1962;2:209–216.
25. Igwé JC, Abia AA, Ibeh CA. Adsorption kinetic and intraparticule diffusivities of Hg, As and Pb ions on unmodified and thiolated coconut fiber. International Journal of Environment Science and Technology. 2008;5(1):83-92.
26. Sousa NVO, Tecia VC, Honorato SB, Gomes CL, Baros FCF, Araujo-Silvia MA, Freire PTC, Nascimento RF. Coconut bagasse treated by thiourea/ammonia solution for cadmium removal: Kinetics and adsorption equilibrum. Biotechnology Resource. 2012;7:1504-1524.
27. Fazal A, Rafique U. Mechanistic understanding of cadmium sorption by sulfonated and esterified spent black tea. International Journal of Chemistry and Environmental Engineering. 2012;3:230-237.
28. Ketcha MJ, Anagho GS, Nsami NJ, Kammegne MA. Kinetic and equilibrium studies of the adsorption of lead (II) ions from aqueous solution onto two Cameroon clays: Kaolinite and smectite. Reserch Journal of Environmental Chemistry and Ecotoxicology. 2011;3:290-297.
29. Eun WS, Rowell RM. Cadmium ion sorption onto lignocellulosic biosorbent modified by sulfonation: The origin of sorption improvement. Chemosphere. 2005;60:1054-1061.
30. Farouq R, Yousef NS. Equilibrium and kinetics studies of adsorption of copper (II) ions on natural biosorbent. International Journal of Chemical Engineering and Applications. 2015;6(5):319-324.
31. Rangabhashiyam S, Anu N, GiriNandagopal MS, Selvaraju N. Relevance of isotherm models in biosorption of pollutants by agricultural by products. Journal of Environmental Chemical Engineering. 2014;6(5):2398-2414.
32. Hamdaouia O, Naffrechoux E. Modeling of adsorption isotherms of phenol and chlorophenols onto granular activated carbon Part I. Two-parameter models and equations allowing determination of thermodynamic parameters. Journal of Hazardous Materials. 2007;147:381-394.
33. Ferrandon O, Bouabane H, Mazet M. Contribution à l'étude de la validité de différents modèles, utilisés lors de l'adsorption de solutés sur charbon actif. Revue des Sciences de l'Eau. 1995;8: 183-200.
34. Tchuifon TDR, Nche GNA, Tchouanyo DH, Ngakou SC, Djoumbissie AL, Anagho SG, Kamgaing T, Ketcha JM. Adsorption studies of methylene blue on methanol modified and unmodified corn stalks and egussi peeling. International Journal of Engineering and Technical Research (IJETR). 2015;3(9):2454-4698.
35. Timur S, Kantradli IC, Ikizoglu E, Yanik J. Preparation of activated carbons from Oreganum stalks by chemical activation. Energy and Fuels. 2006;20(6):2636-2641.
36. Aznar JS. Characterization of activated carbon produced from coffee residues by chemical and physical activation. Master Thesis in Chemical Engineering, Stockholm, Sweden. 2011;66.
37. Maleki A, Mahvi AH, Ehrahimi R, Khan J. Evolution of barley and its ash in removal of phenol from aqueous system. Word Applied Sciences Journal. 2010;8: 369-373.
38. Mareno-Castilla C. Adsorption of organic molecules from aqueous solutions on carbon materials. Carbon. 2004;42:83-94.
39. Tchuifon TDR, Anagho SG, Ndifor-A NG, Ketcha JM. Adsorption of Salicylic and Sulfosalicylic Acid onto powdered activated carbon prepared from rice and coffee husks. International Journal of Current Engineering and Technology. 2015;5(3): 1641-1652.
40. Villacanas F, Fereira MFR, Orfao JJM, Figueiredo JL. Adsorption of simple aromatic compounds on activated carbons. Journal of Colloid and Interface Science. 2006;293:128-136.
41. Alvarez PM, Garcia-Araya JF, Beltran FJ, Masa FJ, Medina F. Ozonation of activated carbons: Effect on adsorption of selected phenolic compounds from aqueous solutions. Journal of Colloid and Interface Science. 2005;283:503-512.
42. Wibowo N, Setyadhi L, Wibowo D, Setiawan J, Ismadji S. Adsorption of benzene and toluene from aqueous

solutions onto activated carbon and its acid and heat treated forms: Influence of surface chemistry on adsorption. Journal of Hazardous Materials. 2007;146:237-242.

43. Newcombe G, Drikas M. Adsorption of NOM activated carbon: Electrostatic and non-electrostatic effects. Carbon. 1997;35: 1239-50.
44. Alberghina G, Bianchini R, Fichera M, Fisichella S. Dimerization of cibacron blue F3GA and other dyes: Influence of salts and temperature. Dyes and Pigments. 2000;46:129-37.
45. Davidson RJ. The Mechanism of gold adsorption on activated charcoal. Journal of the South African Institute of Mining and Metallurgy. 1974;67-76.
46. German-Heins J, Flury M. Sorption of Brilliant Blue FCF in Soils as Affected by pH and Ionic Strength. Geoderma. 2000; 97:87-101.
47. Al-Degs YS, El-Barghouthi MI, El-Sheikh AH, Walker GM. Effect of solution pH, Ionic strength, and temperature on adsorption behavior of reactive dyes on activated carbon. Dyes and Pigments. 2008;77: 16-23.
48. Singh S, Yenkie MKN. Scavenging of priority organic pollutants from aqueous waste using granular activated carbon. Journal of the Chenese Chemistry Society. 2006;53:325-334.
49. Bohli T, Fiol N, Villaescusa I, Ouedemi A. Adsorption on activated carbon from olive stones: Kinetic and equilibrium of phenol removal from aqueous solution. Journal of Chemical Engineering and Process Technology. 2013;4(6):1-5.
50. Li Y, Du Q, Liu T, Peng X, Zhang L. Surface properties of SAC and its adsorption mechanisms for phenol and nitrobenzene. Bioresource Technology. 2012;113:121-126.

Peer-review history:
The peer review history for this paper can be accessed here:
http://www.sciencedomain.org/review-history/23326